

Identification of an Unstable Nonlinear System: Quadrotor

Mauricio Peña, Adriana Luna, Carol Rodríguez

Abstract—In the following article we begin from a multi-parameter unstable nonlinear model of a Quadrotor. We design a control to stabilize and assure the attitude of the device, starting off a linearized system at the equilibrium point of the null angles of Euler (hover), which provides us a control with limited capacities at small angles of rotation of the vehicle in three dimensions. In order to clear this obstacle, we propose the identification of models in different angles by means of simulations and the design of a controller specifically implemented for the identification task, that in future works will allow the development of controllers according to fast and agile angles of Euler for Quadrotor.

Keywords—Quadrotor, model, control, identification.

I. INTRODUCTION

A Quadrotor is an agile and flexible vertical take-off aerial vehicle with capabilities to work in multiple applications such as image recognition [5], [6], [26], agricultural applications [24], military tactics [13] and so on.

Several articles have published many models and controllers implemented in different ways to make motion control of a Quadrotor [25]–[27], being the PhD thesis [10], the most complete and illustrative document on this subject. Other authors we have started from this experience to improve the operating features of the vehicle.

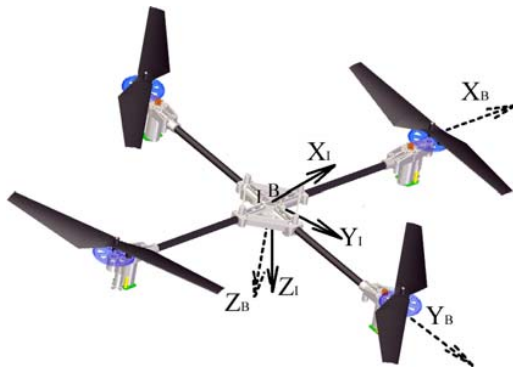


Fig. 1. Reference frame in Quadrotor

In spite of the controllers obtained from analytical models have a good performance, we propose that the controllers designed using experimental models could have better responses since the controller designed is obtained from real values. This article aims to show a simulation case

M. Peña is with the Department of Mechanical Engineering, Libre University, Bogotá, Colombia, (e-mail: mauriciovladimir@gmail.com).

in which mathematical models are based on identification techniques such as parameter estimation and ARX (Auto-Regressive with eXogenous inputs) in order to design controls in different positions and angular velocities to extend the range of operation.

Section II presents a nonlinear model and its linearized model at an equilibrium point. Section III-A shows LQR control with integral effect and its performance, and then it is applied in section IV-B1 where a controller with observer is designed which allows a mathematical solving for the plant that makes possible the model identification from ARX techniques and estimation of parameters given in Section IV-B. Finally, the conclusions raise some observations and suggestions to consider in making identifications of nonlinear and unstable models. [5]–[12], [14]–[17], [22], [23], [27], [28].

II. MATHEMATICAL MODEL

A Quadrotor consists of a central body and four beams joined to it. Each beam has a motor with two rotating wings at the far extreme. The wings give sustentation to the vehicle and offer the possibility of controlling the orientation and translation of the system.

In the identification of nonlinear and unstable systems, as a Quadrotor, it is indispensable to count on some physical knowledge of the system because it helps to understand its unstable behavior when some test signals are introduced.

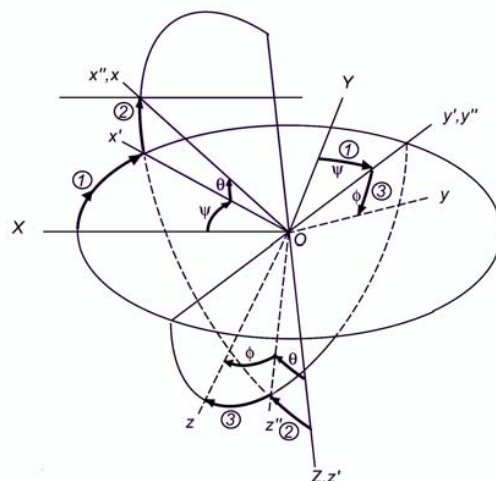


Fig. 2. Definition of Roll, Pitch and Yaw

The dynamic model of the vehicle developing in [18], [21] takes into account the aerodynamic effects of the rotating wings and results in an unstable non-linear system.

Fig. 1 shows the Quadrotor and its reference frame which is represented by the rotational transformation of the Roll-Pitch-Yaw Euler angles as in Fig. 2.

Euler angles - Roll (ϕ), Pitch (θ) and Yaw (ψ) - are defined as reference frames x, y, z rotations around Z, y' and x'' in the amounts ψ, θ and ϕ respectively, as can be seen in Fig. 2.

According to the Newton-Euler equations, the translational and rotational accelerations for the Quadrotor aerial vehicle can be written as in (1):

$$\begin{aligned}
 & \left[\ddot{x} \quad \ddot{y} \quad \ddot{z} \quad \ddot{\phi} \quad \ddot{\theta} \quad \ddot{\psi} \right] = \\
 & \left[\begin{array}{c} \frac{(\sin \phi \sin \psi + \cos \psi \sin \theta \cos \phi) \sum_{i=1}^{i=4} T_i}{m} \\ \frac{(-\cos \psi \sin \phi + \sin \psi \cos \phi \sin \theta) \sum_{i=1}^{i=4} T_i}{m} \\ \frac{mg - \cos \phi \cos \psi \sum_{i=1}^{i=4} T_i}{m} \\ \frac{\dot{\theta} \dot{\psi} (I_{yy} - I_{zz}) + J_r \dot{\theta} \dot{\Omega}_r}{I_{xx}} \\ \frac{\dot{\phi} \dot{\psi} (I_{zz} - I_{xx}) - J_r \dot{\phi} \dot{\Omega}_r}{I_{yy}} \\ \frac{\dot{\phi} \dot{\theta} (I_{xx} - I_{yy}) + J_r \dot{\theta} \dot{\Omega}_r}{I_{zz}} \end{array} \right] + \\
 & \left[\begin{array}{c} \frac{-\sum_{i=1}^{i=4} H_{xi} - C_x \frac{1}{2} A_c \rho \dot{x} |\dot{x}|}{m} \\ \frac{-\sum_{i=1}^{i=4} H_{yi} - C_y \frac{1}{2} A_c \rho \dot{y} |\dot{y}|}{m} \\ \frac{-C_z \frac{1}{2} A_c \rho \dot{z} |\dot{z}|}{m} \\ \frac{l_1 (T_4 - T_2) + \sum_{i=1}^{i=4} (-1)^{i+1} R_{mxi} - l_2 \sum_{i=1}^{i=4} H_{yi}}{I_{xx}} \\ \frac{l_1 (T_1 - T_3) + \sum_{i=1}^{i=4} (-1)^{i+1} R_{myi} + l_2 \sum_{i=1}^{i=4} H_{xi}}{I_{yy}} \\ \frac{l_1 [(H_{x2} - H_{x4}) + (H_{y3} - H_{y1})] + \sum_{i=1}^{i=4} (-1)^i Q_i}{I_{zz}} \end{array} \right] \quad (1)
 \end{aligned}$$

where:

$T_i = C_T \rho A (\Omega_i R)^2$ is the thrust of the i -st propeller, with R is the radius of the propeller and Ω_i is the angular velocity of the i -st propeller.

m is the mass of the vehicle, I_{xx}, I_{yy} and I_{zz} are elements of the inertial momentum matrix, J_r is the inertial momentum of the propellers,

$J_r \omega_{(\phi, \theta, \psi)} \Omega_r$ is the gyroscopic effect of the propeller with respect to the main axes (x, y and z),

H_{xi}, H_{yi} are Hub forces of the i -st propeller,

R_{mxi}, R_{myi} are the roller moments of the i -st propeller,

C_x, C_y and C_z are the drag coefficients,

A_c is the area that the propeller covers,

ρ is the air density,

l_1 and l_2 are the distances between the propeller and the center of the vehicle in the horizontal and vertical plane respectively,

Q_i is the drag momentum produced in the i -st.

For detail description of the model, see [19], [20].

From 1, the equilibrium point X_0 is obtained by equating to zero.

$$X_0 = [0 \quad 0 \quad 0 \quad 0 \quad 0 \quad 0 \quad 0 \quad 0 \quad 0 \quad 0 \quad 0 \quad \psi]^T \quad (2)$$

Any point of equilibrium would mean "hover". The thrust sum must be equal to the weight of the vehicle, so U_0 is a constant. The linear system around the equilibrium point is obtained by using the symbolic toolbox of Matlab:

$$\begin{bmatrix} \dot{v}_x \\ \dot{v}_y \\ \dot{v}_z \\ \dot{\omega}_\phi \\ \dot{\omega}_\theta \\ \dot{\omega}_\psi \end{bmatrix} = \begin{bmatrix} \frac{1}{m} C_t a U_0 (1) \cdot \theta \\ v_x \\ -\frac{1}{m} C_t a U_0 (1) \cdot \phi \\ v_y \\ -\frac{1}{m} C_t a U_0 (1) \\ v_z \\ \frac{1}{I_{xx}} C_t l_1 a U (3) \\ \omega_\phi \\ \frac{1}{I_{yy}} C_t l_1 a U (4) \\ \omega_\theta \\ \frac{1}{I_{zz}} C_q a R U (2) + J_r \dot{U} (5) \\ \omega_\psi \end{bmatrix} \quad (3)$$

where:

C_t is the lift coefficient and C_q is the drag coefficient of the propeller,

$$a = \rho A_c R^2$$

$$U(1) = (\Omega_1^2 + \Omega_2^2 + \Omega_3^2 + \Omega_4^2)$$

$$U(2) = (\Omega_1^2 + \Omega_3^2 - (\Omega_2^2 + \Omega_4^2))$$

$$U(3) = (\Omega_4^2 - \Omega_2^2)$$

$$U(4) = (\Omega_1^2 - \Omega_3^2)$$

$$U(5) = (\Omega_1 + \Omega_3 - (\Omega_2 + \Omega_4))$$

and $U(i)$ are the inputs.

III. CONTROL FOR IDENTIFICATION

For modeling from identification is required to stabilize the plant previously, which can be done with the help of a control in feedback.

Any controller is not the correct to enable identification. It is necessary to obtain a controller that does not erase the dynamics of the plant and if this is simple, the mathematical model of the plant is easy to solve.

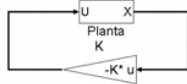


Fig. 3. LQR control for stabilizing the system

A. LQR (Linear Quadratic Regulator)

LQR control ([1]–[3]) is a method to find the optimal solution for a problem of minimization that assures the system stability in close-loop, in addition its calculation is easy. The most general problem that this method can solve is given by the equation of the dynamic system:

$$\dot{x}(t) = A(t)x(t) + B(t)u(t); \quad x(t_0) = x_0 \quad (4)$$

with $x(t) \in R^n$ and $u(t) \in R^m$,

$$z(t) = C(t)x(t) \quad (5)$$

where $A(t)$ is a continuous-time function, $B(t)$ and $C(t)$ are continuous-time and bounded functions. and $z(t) \in R^p$. Equation (6) represents the quadratic cost function to minimize:

$$J = \frac{1}{2} \int_{t_0}^{t_f} [z^T(t)R_{zz}z(t) + u^T(t)R_{uu}u(t)] dt + \frac{1}{2} x^T(t_f)F(t_f)x(t_f)$$

where $R_{zz} > 0$, and $R_{uu} > 0$, are continuous-time and bounded functions defined by the user and $F_{t_f} \geq 0$ refers to a boundary condition.

Thus, the general problem in LQR method is to find an input $u(t)$ in time domain between the initial and final given times. The optimal input is defined by (6):

$$u_{op}(t) = -R_{uu}^{-1}B^T P(t)x(t) = -K(t)x(t) \quad (6)$$

where $P(t)$ (in (7)) is the solution to the Riccati differential equation:

$$-\dot{P}(t) = A(t)^T P(t) + P(t)A(t) + C(t)^T R_{zz} C(t) - P(t)B(t)R_{uu}^{-1}B(t)^T P(t) \quad (7)$$

For linear time-invariant systems, (7) reaches a value in stable state that is reduced to the (8):

$$A^T P + PA + R_{xx} - PBR_{uu}^{-1}B^T P = 0 \quad (8)$$

called the Control Algebraic Riccati Equation (CARE) and it finds the optimum value of P . The optimal input is defined by (9):

$$u(t) = -K_{ss}x(t) \quad (9)$$

The value K_{ss} is easily found by the control system toolbox of Matlab using the syntax: $K_{ss} = lqr(A, B, C^T R_{zz} C, R_{uu})$ ([4]). The diagram that describes the stabilizing control is shown in Fig. 3. Here A , B and C are the matrices associated to the linearized system and R_{zz} and R_{uu} are the weight matrices respectively to increase or to diminish the effect of the states and the entrances and those are selected by the designer in agreement with the required performance.

B. LQR with Integral Effect

Using the concept of the above control we can stabilize the aerial vehicle in hover but we can not follow arbitrary reference angles ϕ , θ and ψ . Thus, it is necessary to add an integral effect. For this aim we can include new states:

$$x_I(t) = \int e(t)dt = \int (r(t) - y(t))dt = \int (r(t) - Cx(t))dt$$

where $e(t)$ is the error signal between the output signal $y(t)$ and the reference signal $r(t)$ given by the user. The new system in state variables is defined by (11):

$$\begin{bmatrix} \dot{x}(t) \\ \dot{x}_I(t) \end{bmatrix} = \begin{bmatrix} A & 0 \\ -C & 0 \end{bmatrix} \begin{bmatrix} x(t) \\ x_I(t) \end{bmatrix} + \begin{bmatrix} B \\ 0 \end{bmatrix} u(t) + \begin{bmatrix} 0 \\ I \end{bmatrix} r(t) \quad (10)$$

$$\begin{bmatrix} B \\ 0 \end{bmatrix} u(t) + \begin{bmatrix} 0 \\ I \end{bmatrix} r(t) \quad (11)$$

With $\bar{x}(t) = [x(t) \ x_I(t)]^T$, the new cost function is defined by (12):

$$J = \int_0^\infty [\bar{x}^T(t)R_{zz}\bar{x}(t) + u^T(t)R_{uu}u(t)] dt \quad (12)$$

therefore:

$$u(t) = - \begin{bmatrix} k & k_I \end{bmatrix} \begin{bmatrix} x(t) \\ x_I(t) \end{bmatrix} = -\bar{K}\bar{x}(t) \quad (13)$$

Once the control has been designed, it must take the shape in the close-loop architecture shown in the diagram by Fig. 4.

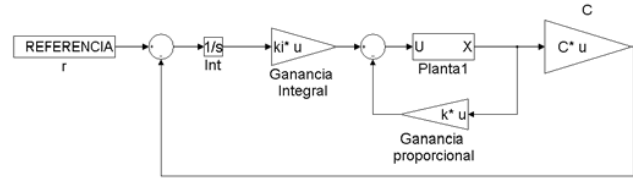


Fig. 4. LQR control following the reference

IV. RESULTS

A. Design of LQR Control

In this section, the values of the parameters are found for a real Quadrotor. A graphic model and the real model are placed in the linear model of the form $\dot{X}(t) = A_{LN}X(t) + B_{LN}U(t)$, with $Y(t) = C_{LN}X(t) + D_{LN}U(t)$, whose values for A_{LN} , B_{LN} , C_{LN} and D_{LN} are:

$$A_{LN} = \begin{bmatrix} 0 & 0 & 0 & 0 & 0 & 0 & 0 & 0 \\ 0 & 0 & 0 & 0 & 0 & 0 & 0 & 0 \\ 0 & 0 & 0 & 0 & 0 & 0 & 0 & 0 \\ 0 & 0 & 0 & 0 & 0 & 0 & 0 & 0 \\ 0 & 0 & 0 & 0 & 0 & 0 & 0 & 0 \\ 0 & 1 & 0 & 0 & 0 & 0 & 0 & 0 \\ 0 & 0 & 1 & 0 & 0 & 0 & 0 & 0 \\ 0 & 0 & 0 & 1 & 0 & 0 & 0 & 0 \end{bmatrix}, \quad B_{LN} = \begin{bmatrix} 0 & 127.4725 & 0 & 0 \\ 0 & 0 & 127.4725 & 0 \\ -7.5188 & 0 & 0 & 278.0868 \\ 0 & 0 & 0 & 0 \\ 0 & 0 & 0 & 0 \\ 0 & 0 & 0 & 0 \\ 0 & 0 & 0 & 0 \\ 0 & 0 & 0 & 0 \end{bmatrix},$$

$$C_{LN} = \begin{bmatrix} 0 & 0 & 0 & 0 & 1 & 0 & 0 & 0 \\ 0 & 0 & 0 & 0 & 0 & 1 & 0 & 0 \\ 0 & 0 & 0 & 0 & 0 & 0 & 1 & 0 \\ 0 & 0 & 0 & 0 & 0 & 0 & 0 & 1 \end{bmatrix} \text{ and } D_{LN} = \begin{bmatrix} 0 & 0 & 0 & 0 \\ 0 & 0 & 0 & 0 \\ 0 & 0 & 0 & 0 \\ 0 & 0 & 0 & 0 \\ 0 & 0 & 0 & 0 \\ 0 & 0 & 0 & 0 \\ 0 & 0 & 0 & 0 \\ 0 & 0 & 0 & 0 \end{bmatrix}$$

With the previous matrices, the weight matrix Q (values of weight for the most important states) and the matrix R (values of weight for the amplitude signal control), the LQR problem

finds the solution with the *lqr* command in control toolbox of Matlab, thus:

$$Q = \begin{bmatrix} 10 & 0 & 0 & 0 & 0 & 0 & 0 & 0 \\ 0 & 10 & 0 & 0 & 0 & 0 & 0 & 0 \\ 0 & 0 & 10 & 0 & 0 & 0 & 0 & 0 \\ 0 & 0 & 0 & 10 & 0 & 0 & 0 & 0 \\ 0 & 0 & 0 & 0 & 10 & 0 & 0 & 0 \\ 0 & 0 & 0 & 0 & 0 & 10 & 0 & 0 \\ 0 & 0 & 0 & 0 & 0 & 0 & 10 & 0 \\ 0 & 0 & 0 & 0 & 0 & 0 & 0 & 10 \end{bmatrix} \text{ and } R = \begin{bmatrix} 1 & 0 & 0 & 0 \\ 0 & 1 & 0 & 0 \\ 0 & 0 & 1 & 0 \\ 0 & 0 & 0 & 1 \end{bmatrix}$$

And the constant matrix of control *k* is calculated. Its value is:

$$k = \begin{bmatrix} 0.00 & -0.00 & 0.00 & -10.22 & 0.00 & -0.00 & 0.00 & -17.45 \\ 10.01 & 0.00 & 0.00 & -0.00 & 17.32 & -0.00 & 0.00 & -0.00 \\ 0.00 & 10.01 & 0.00 & 0.00 & 0.00 & 17.3283 & 0.00 & -0.00 \\ 0.00 & 0.00 & 10.00 & -0.00 & 0.00 & -0.00 & 17.32 & -0.00 \end{bmatrix}$$

$$\text{and } k_i = \begin{bmatrix} 0.0000 & 0.0000 & 0.0000 & -10.0000 \\ 10.0000 & -0.0000 & -0.0000 & -0.0000 \\ 0.0000 & 10.0000 & 0.0000 & 0.0000 \\ 0.0000 & -0.0000 & 10.0000 & -0.0000 \end{bmatrix} \quad (14)$$

The control of the linear system is optimum for these matrices weights *Q* and *R*, so the performance objective for the system is modified by changing these weights to check the signal control is between the limits of the actuator. In the linear system, the dynamic of the four motors (actuators) and the friction forces are despised, while in the non-linear system this dynamics were not despised. Therefore it is in order to compare both systems and to verify that the designed control works appropriately.

The complete architecture of the system including the control is shown in the diagram blocks of Fig. 5 which includes the linear and non-linear systems.

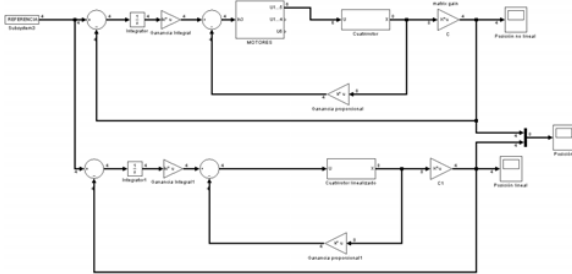


Fig. 5. Block Diagram of the LQR control with integral effect

B. Identification

One of the important parts in the identification process is to have an idea of the bandwidth of the system in open loop from an approximated mathematical model. This bandwidth indicates us the frequencies at which the system should be excited and, if we do not have them, the identification process becomes a process of trial and error, situation in which the resulting models could be simply not predict the dynamics of the system or predict it partially in certain ranges of frequencies.

Neither LQR control nor LQR with integral effect control allow us to isolate the mathematical model of the plant from the model of the system in feedback. Thus, an observer-based controller was necessary.

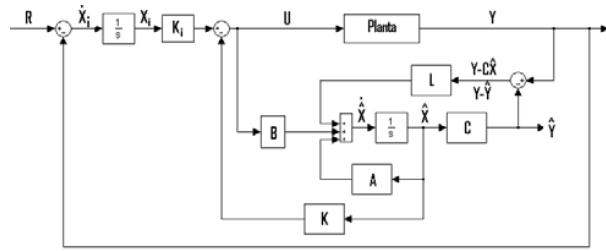


Fig. 6. Block diagram of observer based controller

1. Observer-Based Control

LQR control with integral effect does not allow to find the model of the plant from the identification of the system in feedback, thus a LQR controller with integral effect based on observer must be designed, which can be seen as a controller of two parameters, whose system in feedback allows the algebraic uncovering of the plant of the system as it is mentioned next.

Based on the LQR control with integral effect designed in the previous section, an observer with the objective of reading the states of the system is created.

Fig. 6 can be expressed mathematically as follows:

$$\dot{X}_i = IR - IY$$

$$\dot{\hat{X}} = A\hat{X} + BU + L(Y - C\hat{X}) ; U = -K\hat{X} + K_i X_i$$

where *I* is the identity matrix and *L* is the gains vector of the observer for locating its poles. These poles normally are located at least 6 times further towards the left of the dominant poles in feedback. For the design of this case in particular they were located in $-100, -101, -102, -103, -104, -105, -106, -107$ of so form that the dynamics of the observer is despicable and the system in feedback approaches to order 12 (8 states and 4 integrators of error).

Replacing:

$$\dot{\hat{X}} = A\hat{X} + B(-K\hat{X} + K_i X_i) + L(Y - C\hat{X})$$

$$\dot{\hat{X}} = (A - BK - LC)\hat{X} + BK_i X_i + LY$$

In matricial form:

$$\begin{bmatrix} \dot{\hat{X}} \\ \dot{X}_i \end{bmatrix} = \begin{bmatrix} A - BK - LC & BK_i \\ 0 & 0 \end{bmatrix} + \begin{bmatrix} 0 & L \\ I & -I \end{bmatrix} \begin{bmatrix} R \\ Y \end{bmatrix}$$

$$U = \begin{bmatrix} -K & K_i \end{bmatrix} \begin{bmatrix} \hat{X} \\ X_i \end{bmatrix} + \begin{bmatrix} 0 & 0 \end{bmatrix} \begin{bmatrix} R \\ Y \end{bmatrix}$$

The controller can be seen as a controller of two parameters (Fig. 7)

$$\begin{bmatrix} U_1 \\ U_2 \\ U_3 \\ U_4 \end{bmatrix} = \begin{bmatrix} \bar{G}_{C11} & \dots & \bar{G}_{C14} & \dots & \bar{G}_{C15} & \dots & \bar{G}_{C18} \\ \vdots & \vdots & \vdots & \vdots & \vdots & \vdots & \vdots \\ \bar{G}_{C41} & \dots & \bar{G}_{C44} & \dots & \bar{G}_{C45} & \dots & \bar{G}_{C48} \end{bmatrix} \begin{bmatrix} \bar{R}_1 \\ \vdots \\ \bar{R}_4 \\ \bar{Y}_1 \\ \vdots \\ \bar{Y}_4 \end{bmatrix}$$

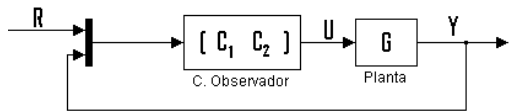


Fig. 7. Block diagram of controller based on observer seen as controller of two parameters.

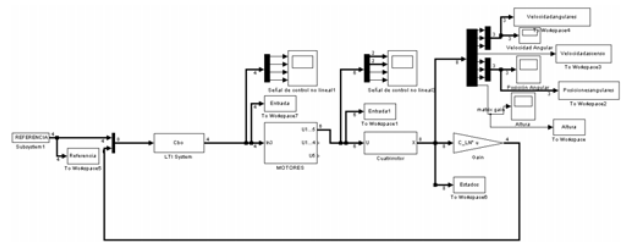


Fig. 8. Block diagram for two parameters control.

$$R = \begin{bmatrix} R_1 \\ R_2 \\ R_3 \\ R_4 \end{bmatrix} = \begin{bmatrix} \phi_r \\ \theta_r \\ \psi_r \\ Z_r \end{bmatrix} \quad Y = \begin{bmatrix} Y_1 \\ Y_2 \\ Y_3 \\ Y_4 \end{bmatrix} = \begin{bmatrix} \phi \\ \theta \\ \psi \\ Z \end{bmatrix} \quad U = \begin{bmatrix} U_1 \\ U_2 \\ U_3 \\ U_4 \end{bmatrix}$$

the system expressed as a controller of two parameters in general form is:

$$U = C_1 R + C_2 Y \tag{15}$$

con:
$$\tag{16}$$

$$Y = GU$$

Thus:

$$Y = G(C_1 R + C_2 Y)$$

$$Y = GC_1 R + GC_2 Y$$

Thus:

$$Y - GC_2 Y = GC_1 R$$

$$[I - GC_2] Y = GC_1 R$$

$$Y = [I - GC_2]^{-1} GC_1 R$$

Thus, the transfer function in feedback is:

$$T = [I - GC_2]^{-1} GC_1 \tag{17}$$

From which the transition function of the plant G is found, thus:

$$[I - GC_2] T = GC_1$$

$$IT - GC_2 T = GC_1$$

$$IT = G [C_1 + C_2 T]$$

$$G = T [C_1 + C_2 T]^{-1} \tag{18}$$

The model of the system remains simple and now its plant is easily cleared.

For the case of the LQR system with integral effect and observer, it starts from the 8 states already mentioned: 6 for the attitude and 2 for the altitude as is shown in Fig. 8.

Continuing with the design of the controller, Fig. 9 shows the responses of the system to inputs of step type. We see that the system follows the references at a finite time.

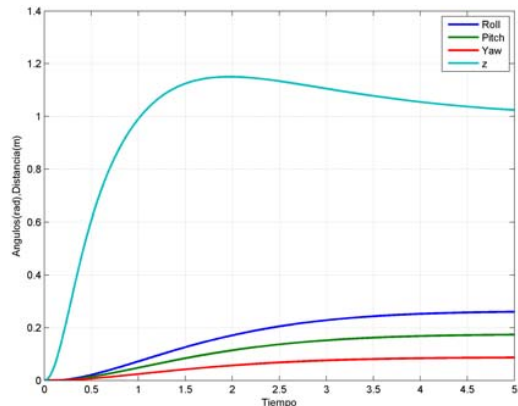


Fig. 9. System responses to reference steps in 0.2618, 0.1745 and 0.087 radians (15, 10 and 5 degrees) in roll, pitch, yaw and 1 meter of altitude respectively.

Taking into account the outputs of the controller are the voltages applied in the motors of propellers (in Volts), we obtained the angular velocities of propellers in rad/s (shown in Fig. 10), and consequently, the thrusts in N and moments in Nm shown in Fig. 11. The control signals do not exceed the conditions of saturation of the actuators as is observed in Fig. 10 and Fig. 11.

Starting from the nonlinear model of the plant, we linearized it around of an equilibrium point and then, the crossover frequency of gain of the system in open loop is taken from its diagram of Bode. We designed a controller such that the crossover frequency of gain of the system in feedback is smaller or just equal than the crossover frequency of gain in openloop for keeping the dynamics of the plant since the primary target of the control is to make insensitive the dynamics input-output of the system in feedback to parametric variations of the plant.

The previous statements can be observed in the theorem of Black, written for systems MIMO with L , F , S (sensitivity function) and T (function of complementary sensitivity).

$$L = GK$$

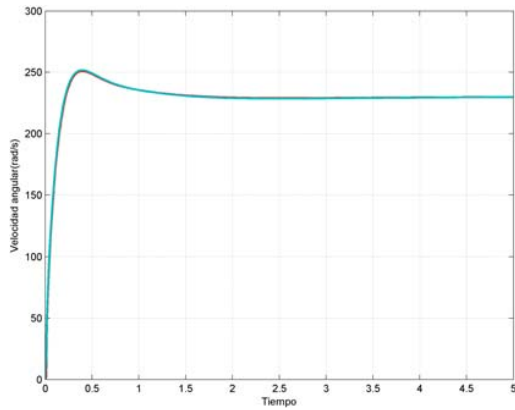
$$F = I + GK$$

$$S = (I + GK)^{-1}$$

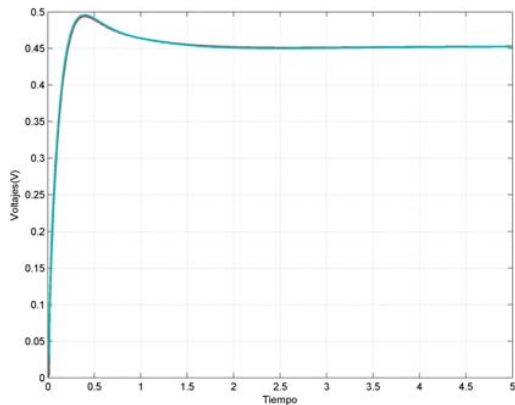
$$T = PK(I + GK)^{-1}$$

that it affirms: The influence of the disturbances is attenuated in a system in feedback if:

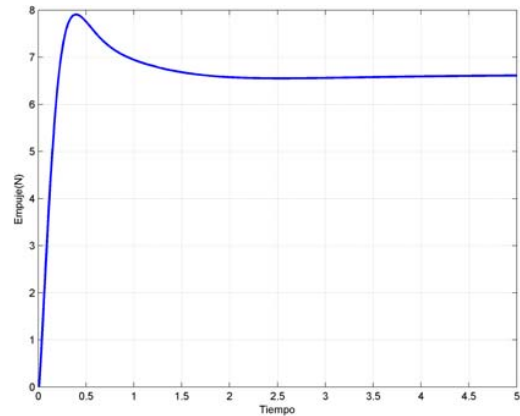
$$|L| \gg 1, \quad |F| \gg 1$$



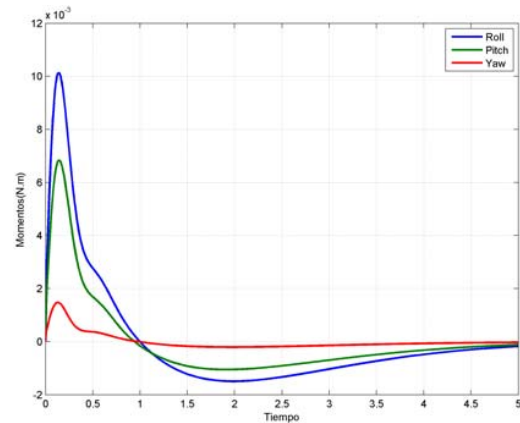
(a) Angular Velocity of the propellers.



(b) Voltage in the power circuit.



(a) Thrust generated for the propellers.



(b) Moments in the system.

Fig. 10. Control signal in the actuators.

Fig. 11. Control signal for the actuators.

and

$$S \approx 0$$

In other words, the changes of the system G in openloop will be less perceivable than the changes of the system in feedback T .

As the plant in feedback is non observable since it has a realization in another space, the result of the identification in black box produces a matrix such that the outputs are a linear combination of state variables without an associated physical sense to the plant.

2. Identification Using Controller Based on Observer

As the real system is nonlinear, we expect that there is no an unique linear model that describes it. Thus, we do the identification of the plant and obtain the performance of the process in Fig. 12.

In Fig. 12 we observe four set data, *datav*, *m0*, *m1*, *m2*. The first one is the simulated data, and the next ones are models obtained by PEM, ARX and NLARX respectively. We analyze that any of the three methods of identification predicts accurately the behavior of the control-plant system in feedback. The dynamics of the plant can be found by using 18.

From the models *m0* and *m1* (obtained by means of PEM and ARX respectively) the equations of the system are obtained in form of equations of variables of state of 50 states, that are indispensable to reduce them without losing considerable information in the frequencial rank, where the dynamics of system is predominant. The models were reduced by using singular values of Hankel with the command *reduce* of MATLAB, later the validity of these models is corroborated comparing them with the nonlinear system in the dominion of the time.

The differences between the models are observed in the Fig. 13 by zooming, otherwise they would not notice. The Fig. 13 shows the responses of the system: nonlinear, simulated linear system G_{ss} , identified system by PEM G_0 , reduced identified system by PEM G_{0red} , identified system by ARX G_1 and reduced identified system by ARX G_1 . Any of these two models of plant would correctly describe the dynamics of the airship, at least in the dominion of the time.

On top of that, the frequency response of the linearized system is observed in the Fig. 14, both models obtained by means of identification using algorithms PEM and ARX of high order and models PEM and ARX of reduced orders is compared. It is possible to determine that they are

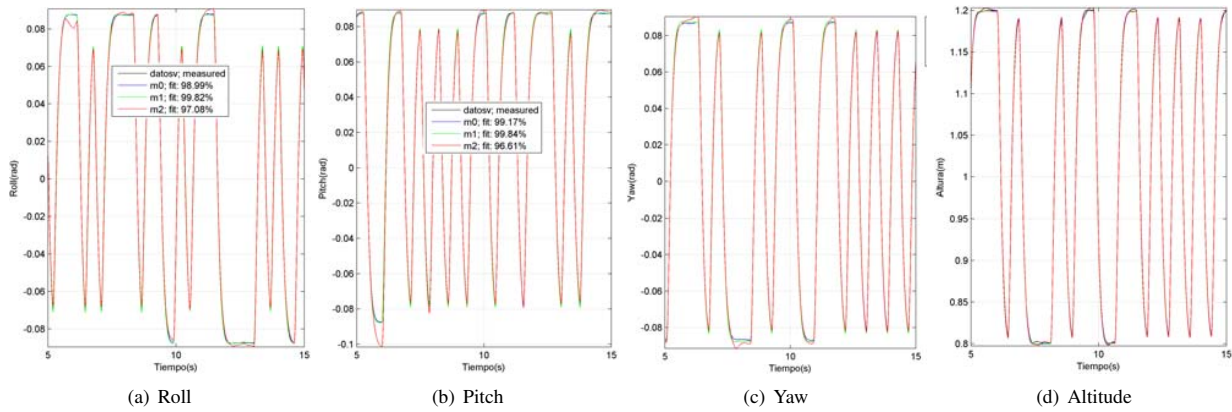


Fig. 12. Fitness of the identified models by using a PRBS (Pseudo Random Binary Signal).

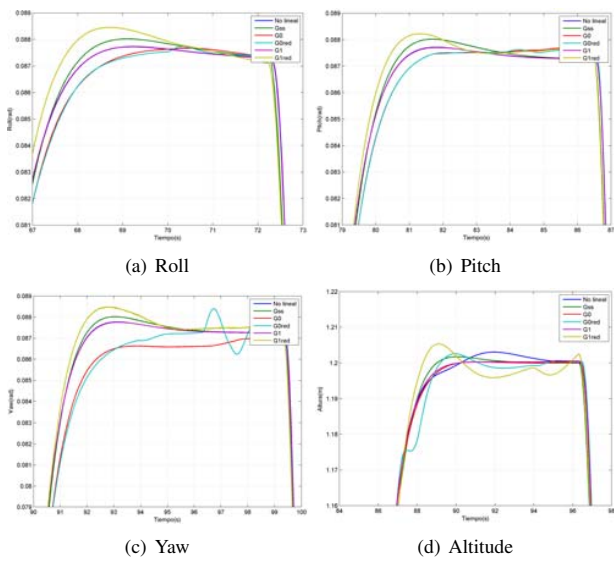


Fig. 13. Comparison among the responses of the nonlinear system, system with identified plant and system with identified plant reduced.

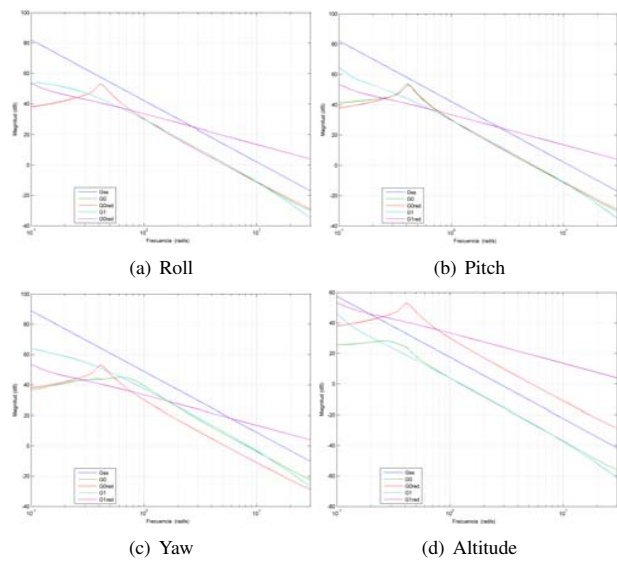


Fig. 14. Comparison between the frequency responses of the linearized model, model with identified plant and model with identified plant reduced.

approximated in the rank of 10^0 to 10^2 rad/s where the predominant dynamics of the system is had.

Analyzing and verifying the validity of these models, we can be certain that they are useful in the description of the plant: either to control and dynamic system analysis or for a further investigation of a improved and/or extended design of a Quadrotor.

Despite the range in which the linearized model is sufficient to perform control on the vehicle, other angular positions can be taken to identify others models in order to the Quadrotor can travel at higher speeds in the horizontal plane and with better maneuverability.

Maintaining the signal of excitation in the height reference and changing the signals of excitation in the references of Roll, Pitch and Yaw in the same amounts. Linearized models were obtained whose satisfactory results are in [18].

To illustrate, the model obtained by PEM in equations

matrix of state variables A , B , and D is:

$$A = \begin{bmatrix} 0.2637 & 1.0586 & -0.3342 & -0.1575 & 0.6655 & 0.0348 \\ -0.4457 & 0.2637 & -0.2009 & 0.0546 & 0.1302 & 0.1937 \\ 0 & 0 & 0.0361 & 0.2128 & 0.1827 & 0.0861 \\ 0 & 0 & -0.7769 & 0.0361 & -0.0772 & 0.0236 \\ 0 & 0 & 0 & 0 & 0.1244 & -0.1970 \\ 0 & 0 & 0 & 0 & 0.8348 & 0.1244 \\ 0 & 0 & 0 & 0 & 0 & 0 \\ 0 & 0 & 0 & 0 & 0 & 0 \\ 0 & 0 & 0 & 0 & 0 & 0 \\ 0 & 0 & 0 & 0 & 0 & 0 \\ 0 & 0 & 0 & 0 & 0 & 0 \\ 0 & 0 & 0 & 0 & 0 & 0 \\ 0 & 0 & 0 & 0 & 0 & 0 \\ 0 & 0 & 0 & 0 & 0 & 0 \\ 0 & 0 & 0 & 0 & 0 & 0 \\ 0 & 0 & 0 & 0 & 0 & 0 \\ 0 & 0 & 0 & 0 & 0 & 0 \\ 0 & 0 & 0 & 0 & 0 & 0 \\ 0 & 0 & 0 & 0 & 0 & 0 \\ 0 & 0 & 0 & 0 & 0 & 0 \\ 0 & 0 & 0 & 0 & 0 & 0 \end{bmatrix}$$

$$B = \begin{bmatrix} -0.0437 & 0.2541 & 1.2324 & -14.0937 \\ -0.0372 & -3.4209 & 0.5442 & -17.9142 \\ 0.0023 & 0.3407 & -0.0617 & 7.9305 \\ -0.0842 & -0.8811 & -0.8173 & 2.4644 \\ -0.0355 & 3.4869 & 0.0815 & -1.4586 \\ 0.0430 & -1.1115 & -0.8651 & 1.0147 \\ -0.0299 & -0.7688 & -0.6186 & -13.28 \\ -0.0279 & -2.2966 & -0.5460 & -4.7082 \\ -0.2091 & -0.2156 & -0.2683 & -4.6788 \\ -0.0212 & -2.4429 & 5.4089 & -1.2185 \\ -0.0189 & -2.4560 & 2.9797 & -1.1907 \\ 0.0367 & -5.9319 & -5.3715 & -1.1438 \end{bmatrix}$$

$$C = \begin{bmatrix} 0.5452 & -0.1174 & -1.3459 & 1.1945 & 2.1627 & 2.65373 \\ -0.2423 & -0.2435 & -2.4417 & 0.8565 & -1.4513 & 1.1402 \\ -2.7313 & 0.6462 & -0.4365 & -0.0985 & 0.538351 & 0.2496 \\ 0.1619 & 1.4412 & 3.7846 & 0.6537 & -2.5137 & -0.9570 \end{bmatrix}$$

$$\begin{bmatrix} -0.9076 & -0.1814 & -0.1845 & 1.1370 & -0.3952 & 0.607 \\ 0.3083 & -2.3451 & 0.4517 & -0.5037 & 0.4335 & -0.3355 \\ 0.4213 & -0.1691 & -0.2003 & 0.3096 & 0.1068 & -0.1659 \\ -0.9621 & -3.5122 & -0.8971 & -1.1906 & 0.8778 & 0.0702 \end{bmatrix}$$

$$D = \begin{bmatrix} 0 & 0 & 0 & 0 \\ 0 & 0 & 0 & 0 \\ 0 & 0 & 0 & 0 \\ 0 & 0 & 0 & 0 \end{bmatrix} \quad (19)$$

V. CONCLUSIONS

For identification process, controllers are not designed in order to fulfill performance characteristics or improve response speeds. The controls in feedback are designed of such a form that is possible to extract the dynamics of the plant. This means that the dynamic response of the control does not have to hide the dynamics of the plant, whereas the objective of an ideal control is to erase the dynamics of the plant.

If a model of the plant is had and the operation limits of the actuators are known, control strategies can be designed that allow to obtain an optimal performance of the system.

The identification process is very specific for the Quadrotor, this is a nonlinear and unstable plant, that is why its identification in openloop is impossible. It is necessary, first of all, to stabilize the plant with some type of control in feedback that does not hide the dynamics of the plant and in addition that it can make observable the system in order to be able to obtain the model of the plant. Having some idea of the bandwidth of the system is very important to excite and identify the system by using test signals, since by using methods of test and error, it can be imprecise and belated, which could cause that the resulting models simply are not able to predict the dynamics of the system or partially predict it in certain ranges of frequencies. This is obtained by studying a mathematical model with physical sense of the plant that perhaps does not contain the totality of variables and parameters that perfectly describe the plant, but that contains the important phenomena of its dynamics.

REFERENCES

- [1] *Ingenieria de control moderno*. Pearson, 1994.
- [2] *Modelling of Dynamic Systems*. Prentice Hall PTR, 1994.
- [3] *Feedback Systems: An introduction for Scientists and engineers*. Princeton univ, 2006.
- [4] *System Control toolbox*. Mathworks, 2006.
- [5] J.P. Mahony R. Altug, E. Ostrowski. Control of a quadrotor helicopter using visual feedback. In IEEE, editor, *Proceedings of the International Conference on Robotics and Automation*, volume 1, pages 72–77. IEEE, August 2002.
- [6] J.P. Mahony R. Altug, E. Ostrowski. Quadrotor control using dual camera visual feedback. In IEEE, editor, *Proceedings of the International Conference on Robotics and Automation*, volume 3, pages 4294–4299. IEEE, September 2003.
- [7] P. Siegwart R. Bouabdallah, S. Murrieri. Design and control of an indoor micro quadrotor. In IEEE, editor, *Proceedings of the International Conference on Intelligent Robots and Systems*, volume 5, pages 4393–4398, April 2004b.
- [8] P. Siegwart R. Bouabdallah, S. Murrieri. Pid vs lq control techniques applied to an indoor micro quadrotor. In IEEE, editor, *Proceedings of the International Conference on Intelligent Robots and Systems*, volume 3, pages 2451–2456. September 2004c.
- [9] P. Siegwart R. Bouabdallah, S. Murrieri. Backstepping and sliding-mode techniques applied to an indoor micro quadrotor. In IEEE, editor, *Proceedings of the International Conference on Robotics and Automation*, pages 2247–2252, April 2005a.
- [10] S. Bouabdallah. *Design and control of quadrotors with application to autonomous flying*. PhD thesis, Ecole Polytechnique Federale de Lausanne, 2004a.
- [11] Pierpaolo Murrieri Bouabdallah S. and Roland Siegwart. Towards autonomous indoor micro vtol. *Autonomous Robots*, 18(2):171–183, March 2005b.
- [12] Dzul A. Lozano R. Castillo, P. Real-time stabilization and tracking of a four-rotor mini rotorcraft. *IEEE Transactions on Control Systems Technology*, 12(4), 2004.
- [13] J. Cycon D. Murphy. Applications for mini vtol uav for law enforcement. In *SPIE Proc. 3577: Sensors, C3I, Information, and Training Technologies for Law Enforcement*, November 1998.
- [14] M. Labonte G. Dunfied, J. Tarbouchi. Neural network based control of a four rotor helicopter. In *IEEE International Conference on Industrial Technology*, 2004.
- [15] Lagoa C.M. Wang Q. Ray A. Horn J.F., Tolani D.K. Probabilistic robust control of rotorcraft. *Control Engineering Practice* 13, 2005.
- [16] Wu C.J. Lai L.C., Yang C.C. Time-optimal control of a hovering quadrotor helicopter. *Journal of Intelligent and Robotic Systems*, 2006.
- [17] P McKerrow. Modelling the draganflyer four-rotor helicopter. In *IEEE International Conference On Robotics And Automation*, 2004.
- [18] Mauricio Vladimir Pe na. Modelamiento, simulación y hallazgo de modelos linealizados a partir de técnicas de identificación de un cuatrirrotor. Master's thesis, National University of Colombia, 2009.
- [19] Ramirez R Peña G, Sofrony J. Dynamic model of a four rotor flying vehicle. In *11th Pan-American Congress of Applied Mechanics - PACAM XI*, volume 1, Foz de Iguacu, Brazil, 2009.
- [20] Rodríguez C. Peña G Mauricio, Vivas C. Modeling and lqr control of a quadrotor. *Revista Avances*, 2010.
- [21] Rodríguez F Carol Peña G Mauricio, Vivas G Carlos. Simulation of the quadrotor controlled with lqr with integral effect. In *Proceedings of the COBEM 2011 - 21st International Congress of Mechanical Engineering*, October 2011.
- [22] Corke P. Pounds P., Mahony R. Modelling and control of a quad-rotor robot. *Australian National University*, 2002.
- [23] P Hynes J Roberts Pounds P., R Mahony. Design of a four-rotor aerial robot. In *Proceedings of the 2002 Australasian Conference on Robotics*, pages 145–150, November 2002b.
- [24] S.E. Dunagan R.G. Higgins D.V. Sullivan J. Zheng B.M. Lobitz J.G. Leung B.A. Gallmeyer M. Aoyagi R.E. Slye d J.A. Brass S.R. Herwitz, L.F. Johnson. Imaging from an unmanned aerial vehicle: agricultural surveillance and decision support. In *Computers and Electronics in Agriculture*, volume 44, 2004.
- [25] H. Wang H.O. Tanaka, K. Ohtake. A practical design approach to stabilization of a 3-dof rc helicopter. *IEEE Transactions on Control Systems Technology*, 2004.
- [26] JP How E Feron Tournier, M Valenti. Estimation and control of a quadrotor vehicle using monocular vision and moire patterns. In AIAA Guidance, editor, *Navigation and Control Conference*, 2006.
- [27] Holger Voos. Nonlinear and neural network-based control of a small four-rotor aerial robot. *IEEE Transactions on Control Systems Technology*, 12(4), 2007.
- [28] Schlaile C. Trommer G. F. Wendel J., Meister O. An integrated gps/mems-imu navigation system for an autonomous helicopter. In *Aerospace Science and Technology*, 2006.

Mauricio Peña Mechanical Engineering. M.Eng. Industrial Automation. PhD student of Mechanical Engineering. Researcher and Associated Teacher at the Universidad Libre, Colombia.

Adriana Luna Electronical Enginnering. M.Eng. Industrial Automation.
Researcher and Associated Teacher at the Universidad Libre, Colombia.

Ivonn Rodríguez Electronical Enginnering. M.Eng. Industrial Automation.
Researcher and Associated Teacher at the Universidad Libre, Colombia.